

國立臺灣大學理學院地質科學系暨研究所

碩士論文

Institute of Geosciences

College of Sciences

National Taiwan University

Master Thesis

不知道怎麼排兩個 advisor

National Taiwan University (NTU) Thesis

陳季晴

Ji Ching Chen

指導教授: 譚諤 博士

Advisor: Eh Tan Ph.D.

中華民國 111 年 5 月

May, 2022

國立臺灣大學碩士學位論文

口試委員會審定書



不知道怎麼排兩個 advisor

National Taiwan University (NTU) Thesis

本論文係陳季晴君（R09224122）在國立臺灣大學地質科學系暨研究所完成之碩士學位論文，於民國 111 年 5 月 1 日承下列考試委員審查通過及口試及格，特此證明

口試委員：_____

（指導教授）

_____	_____
_____	_____
_____	_____
_____	_____

所 長：_____

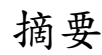


Acknowledgements

還沒有





[illegible]

關鍵字：中文、論文



Abstract

Abstract

Keywords: LaTeX, Thesis



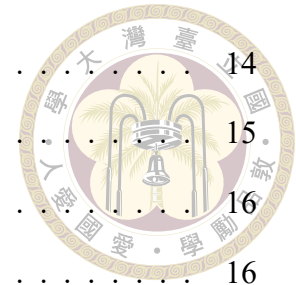




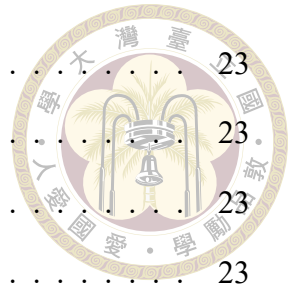
Contents

	Page
Verification Letter from the Oral Examination Committee	i
Acknowledgements	iii
摘要	v
Abstract	vii
Contents	ix
List of Figures	xi
List of Tables	xiii
Denotation	xv
Chapter 1 Introduction	1
1.1 Background	1
1.2 Review of flat subduction numerical models	2
1.3 Motivation	5
1.4 Geophysical observation in Cocos subduction zone	5
1.5 Summery	5
Chapter 2 Numerical modelling method	7
2.1 Governing equation	7
2.1.1 Continuum—Conservation of mass	7
2.1.2 Motion—Conservation of momentum	11
2.1.3 Heat equation — Conservation of energy	14
2.2 Finite elements method	14

2.3	Rheological behavior	14
2.4	Phase change	15
2.4.1	Peridotite — Serpentinite	16
2.4.2	Basalt — Eclogite	16
2.4.3	Sediment — Schist	17
2.4.4	Hydrated olivine — Peridotite	17
2.5	Boundary condition	18
2.5.1	Kinematic boundary condition	18
2.5.2	Thermal boundary condition	18
2.6	FLAC	18
2.7	Initial Model	19
Chapter 3	Numerical model result	21
3.1	Reference model	21
3.2	Flat subduction definition	21
3.3	Oceanic lithosphere	21
3.3.1	Oceanic plateau	21
3.3.2	Basalt transformation	21
3.4	Continental lithosphere	21
3.4.1	Thickness	21
3.4.2	Thermal state	21
3.4.3	lithosphere strength	21
3.5	Sublithosphere mantle	21
3.5.1	Viscosity	21
3.5.2	Serpentinization	21
3.5.3	410 discontinuity	21
Chapter 4	Discussion	23
4.1	Type of flat subduction	23



4.2	Magma sources of flat subduction	23
4.3	Serpentinization and observation	23
4.4	Flat subduction in Mexico	23
4.5	Flat subduction in Chile	23
4.6	Shallow angle subduction	23
References		25
Appendix A — Introduction		25
A.1	Introduction	25
A.2	Further Introduction	25
Appendix B — Introduction		27
B.1	Introduction	27
B.2	Further Introduction	27







List of Figures

Figure 2.1	Eulerian (a) and Lagrangian (b) elementary volumes considered for the derivation of continuity equation.	8
Figure 2.2	Lagrangian elementary Volume considered for the derivation of the respective form of x-momentum equation.	12
Figure 2.3	Elastic deformation	15
Figure 2.4	Phase diagram showing the stability field for mafic rocks (Hacker et al., 2003).	17





List of Tables





Denotation

E	能量
m	質量
c	光速
P	概率
T	時間
v	速度
勸學	君子曰





Chapter 1 Introduction

1.1 Background

Geosynclinal theory was one of the famous theory in the geological studies history. It was believed that the earth's crust deformed with vertical motion in each geoloical zone while the Plate tectonic theory claimed that the earth's crust deformed with horizontal motion. In Geosynclinal theory, geological zone occurred weathering, magmatism and matamporphism process during geological time scale. Since 1960s, geophysics was revolutionized by the discovery of plate tectonics, that is, the plate tectonic theory had been proposed. The heat heterogeneous in earth's interior lead to gravitational instability, and therefore the earth's surface manifestations as plate tectonics (Jordan, 1978). The plate tectonic theory first defined the uppermost layers which is outside the upper thermal boundary layer — lithosphere which consist with crust and part of mantle. Since lithosphere broken into many plate, horizontal motion dominate the Earth's surface with tectonic deformation processes occur in plate boundary. The convergent boundaries represented by the trench and subduction zone where one of the plate destroyed. The divergent boundaries represented by the mid-ocean-ridge system where plate produced. The transform faults as a famous example of which plates move laterally relative to each other (The solid earth, 2005).

In the convergent plate boundary, the thermal state of old lithosphere is relative colder than the ambient mantle, which lead to a denser condition. The cold region is enough to generate a gravitational instability in the subduction zone. Therefore, the heavy


lithosphere develop the trench and sink into mantle which is so-called "slab". The main changes which occur in the subducting plate are the shallow reaction of the oceanic crust to eclogite and the changes deeper in the mantle of olivine to a spinel structure and then to post-spinel structures. Phase changes result in increases in the density of the subducting slab. In the meantime, slab remains cold with gravitational instability. Thermal contraction provides the greatest contribution to the overall driving force. (The solid earth, 2005; Turcotte and Schubert, 2002). The geometry of slab varies considerably on Earth, with variations in slab dip angle and bending curvature (Schellart, 2020).

Flat subduction is a trickier circumstances of subduction geometry. In the flat subduction area, a part of the slab attains a horizontal orientation for several hundred kilometers below the overriding plate while the others part of the slab sinks into the mantle with a normal slab dip.

1.2 Review of flat subduction numerical models

目前造成平坦隱沒發生的機制眾說紛紜。南美洲區域平坦隱沒的發生區域與隱沒的中洋脊有幾何上的相關性，海洋地殼上中洋脊與海洋高原的存在可能會導致總體密度較低、浮力較大，因此過去曾經隱沒的中洋脊被認為是造成平坦隱沒的主要原因。


Hunen et al., 2002 最早將模型加入增厚的海洋地殼，以模擬過去智利與秘魯曾經有中洋脊與海洋高原進入隱沒帶中的紀錄。增厚海洋地殼有較低的密度與較大的浮力，其上方岩相需要比原先更大的壓力與更高的溫度才會從玄武岩相變成密度高的榴輝岩，可能使隱沒板塊與周遭地幔沒有顯著密度差而發生平坦隱沒。不過由於該研究模型僅二維，單純加入增厚海洋地殼所呈現的模型雖然能呈現平



坦隱沒，但結果是假設第三維上有無限延伸的增厚海洋地殼，現實中增厚的海洋地殼能造成的浮力效應應遠小於二維模型中的結果。Florez-Rodríguez et al., 2019。在三維模型中證明了這一點，他們提出若將現在自然界中最大的洋脊隱沒進入地幔，其所提供的浮力也只會造成海洋板塊傾角減少原先的 10 度。若從自然界中來看，確實有許多區域皆有海脊隱沒的證據，例如勘察加半島 (Kamchatka) 有皇帝海脊 (Emperor Ridge) 隱沒、琉球 (Ryukyu) 有大東海脊 (Daito Ridge) 隱沒以及馬里亞納 (Mariana) 與馬庫斯—內克海脊 (Marcus-Necker Ridge) 隱沒，然而只有秘魯與智利有平坦隱沒的特徵。此外，在墨西哥有平坦隱沒的特徵，然而墨西哥沒有任何海脊或海洋高原的隱沒紀錄，因此增厚的海洋地殼發生平坦隱沒的理論近年來逐漸站不住腳 (Schellart, 2020)。

Huneeuw et al., 2000 使用二維笛卡爾座標數值模型進行秘魯與智利平坦隱沒的模擬。在他們的模型中，唯一能成功演化出平坦隱沒的機制只有海溝後撤迫使大陸岩石圈逆衝到隱沒板塊之上。Liu and Currie, 2016 使用二維模型模擬過去股法拉隆板塊板塊的平坦隱沒機制，他們加入增厚的海洋地殼後並無法觸發平坦隱沒的產生，然而，再加入額外大陸岩石圈的水平速度後，平坦隱沒便能成功再現。Axen et al., 2018 使用同樣的數值模型將古代北美西部的克拉通放置於大陸板塊前，成功模擬出增厚海洋地殼加上快速移動大陸岩石圈能發生平坦隱沒，並且能將克拉通從大陸岩石圈底部刮除，證實了平坦隱沒能破壞大陸岩石圈。在該研究中並沒有考慮克拉通對平坦隱沒的影響。

Manea et al., 2012 提出了另外的看法。他們利用三維模型模擬過去 30Ma 以來智利區域的隱沒帶動態行為，使用額外施加的邊界條件強迫智利海溝後撤，發現海溝後撤能夠施加給隱沒板塊的地幔流吸力 (suction) 不足以讓巨大厚重的海洋板塊變平坦，因此他們在模型上覆板塊加上克拉通，系統性測試從 150-300 公里



厚的大陸岩石圈與海溝距離 600-1000 公里時隱沒帶下方地幔流產生的動力壓力 (dynamic pressure)。他們發現在只有在克拉通與海溝距離約 800 公里且克拉通厚度大於 200 公里時平坦隱沒才會生成。當他們把造成海溝後撤的邊界力移除時，不會觸發平坦隱沒的形成，因此他們得出的結論是需要同時有海溝後撤與克拉通的存在才會觸發平坦隱沒。這是首次將克拉通加進數值模型裡的山根平坦隱沒模型。隨後 Liu and Currie, 2016 效仿同樣的機制，將過去普遍認為存在於北美板塊西部下方的科羅拉多高原山根放入模型中，模擬古法拉龍板塊平坦隱沒演化。他們認為克拉通與山根的存在只是加快平坦隱沒的形成，但真正觸發平坦隱沒的機制是增厚海洋地殼延緩玄武岩相變成榴輝岩。Hu et al., 2016 使用三維模型 CitcomS 模擬整個南美洲海溝 45 Ma 以來隱沒帶演化。在加入克拉通的模型中，隱沒板塊傾角有降低的趨勢，不過根據模型結果，真正造成平坦隱沒的形成依然與隱沒海脊相關，只有在海脊進入三維模型後隱沒傾角才出現顯著降低。

因此，目前的平坦隱沒數值模型大多以擬合智利、祕魯與法拉龍板塊為主，觸發平坦隱沒的機制大多與克拉通的存在與否、是否有洋脊隱沒以及上覆板塊的移動速度為主要測試，墨西哥區域尚未有平坦隱沒的數值模型被提出。在墨西哥，隱沒板塊上沒有任何增厚的紀錄，此外該地區北美板塊移動速率遠低於南美洲與過去法拉龍板塊隱沒時期的北美板塊，因此墨西哥區域的山根平坦隱沒機制尚未有統一定論。本研究期待能利用數值模擬得到墨西哥平坦隱沒從過去 50 Ma 以來的演化，並提出新的演化機制模型，填補過去尚未成熟的平坦隱沒機制理論。

1.3 Motivation

1.4 Geophysical observation in Cocos subduction zone

1.5 Summery







Chapter 2 Numerical modelling method

Since the subduction process contain slow deformation and the constrain for deep lithosphere evolution is not well understand from either geophysical observation in depth or geology study in time, computer model is a suitable way to study subduction zone, especially the numerical model. While the analytic solution is hard to solve, numerical model has become a useful method for studying Earth evolution.

The numerical models in this study address the dynamics process of flat subduction, in which an oceanic plate subducts beneath continental plate. The goal of this work is to address the controls on subducting plate dynamics and to determine the conditions under which flat subduction may develop.

In this chapter, we introduce the method of numerical model and the initial model setup. In section 2.1, we discuss the governing equations. In section 2.2, the finite elements method will be briefly discuss. The material properties, phase transition and model boundary conditions are given in section 2.3 ,2.4 and 2.5, respectively. In section 2.6, we introduce the Fast Lagrangian Analysis of Continua technique. In section 2.7, the model geometry is presented.

2.1 Governing equation

2.1.1 Continuum—Conservation of mass

In geodynamics modelling, we consider major rock units as continuous geological media. The continuous description is described by field variables such as density, pressure,

velocity, strain, etc. The continuity can be transformed into quantitative mathematical formalism, that is, continuity equation.



The mass conservation equation in Lagrangian form is as follow

$$\frac{\partial \sigma_{ij}}{\partial x_j} + \rho g_i = \rho \frac{\partial D_{vi}}{\partial t} \quad (2.1)$$

A Lagrangian points is strictly connected to a single material point and is moving with this point. Therefore, the same material point is always in same coordinate independent of the moment of time. On the other hand, Eulerian point is an immobile point. The proof of eq.(2.1) is as follow

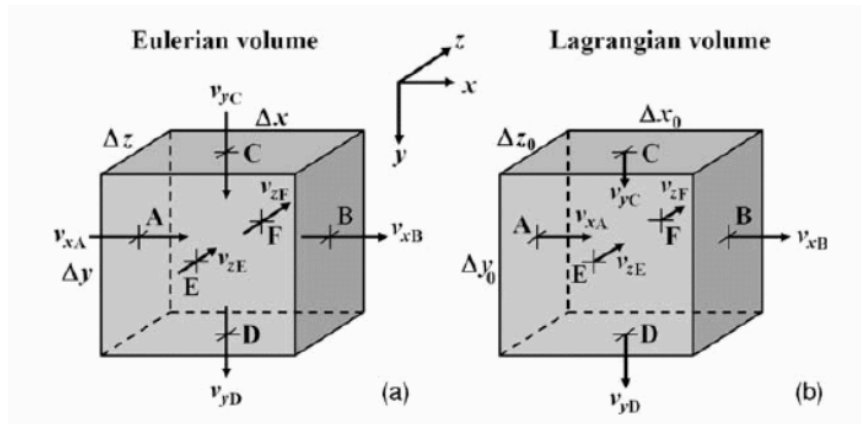


Figure 2.1: Eulerian (a) and Lagrangian (b) elementary volumes considered for the derivation of continuity equation.

Since the volume is always related to the same material points, the amount of mass in the moving Lagrangian volume remains constant. However, the volume change due to the internal expansion or contraction process. The initial average density ρ_0 in a Lagrangian volume (V_0) is given by:

$$\rho_0 = \frac{m}{\Delta x_0 \Delta y_0 \Delta z_0} \quad (2.2)$$

After a small period of time (Δt), the Lagrangian volume undergo internal process, thus the volume become V_1 and the average density change to:

$$\rho_1 = \frac{m}{\Delta x_1 \Delta y_1 \Delta z_1} \quad (2.3)$$

Lagrangian material in time derivative is:

$$\frac{D\rho}{Dt} \approx \frac{\Delta\rho}{\Delta t} = \frac{\rho_1 - \rho_0}{\Delta t} = \frac{m}{\Delta x_1 \Delta y_1 \Delta z_1 \Delta t} - \frac{m}{\Delta x_0 \Delta y_0 \Delta z_0 \Delta t} \quad (2.4)$$

The relationship between new and old dimensions of Lagrangian volume is base on the relative movements of the volume's boundary, the displacement is equal to the velocity times period of duration:

$$\Delta x_1 = \Delta x_0 + \Delta t \Delta v_x \quad (2.5)$$

$$\Delta y_1 = \Delta y_0 + \Delta t \Delta v_y \quad (2.6)$$

$$\Delta z_1 = \Delta z_0 + \Delta t \Delta v_z \quad (2.7)$$

By using the equation above (2.5-2.7), replace the Δx_1 , Δy_1 , Δz_1 to eq 2.4:

$$\frac{D\rho}{Dt} \approx \frac{\Delta\rho}{\Delta t} = \frac{m\Delta x_0 \Delta y_0 \Delta z_0 - m\Delta x_1 \Delta y_1 \Delta z_1}{\Delta x_1 \Delta y_1 \Delta z_1 \Delta t \Delta x_0 \Delta y_0 \Delta z_0} \quad (2.8)$$

Since $\Delta x_0 \Delta y_0 \Delta z_0 = \rho_0$, the following expression can be obtain:

$$\frac{\Delta\rho}{\Delta t} + \rho_0 \frac{\frac{\Delta v_x}{\Delta x_0} + \frac{\Delta v_y}{\Delta y_0} + \frac{\Delta v_z}{\Delta z_0} + K_1}{K_2} = 0 \quad (2.9)$$

$$K_1 = \Delta t \left(\frac{\Delta v_x}{\Delta x_0} \frac{\Delta v_y}{\Delta y_0} + \frac{\Delta v_x}{\Delta x_0} \frac{\Delta v_z}{\Delta z_0} + \frac{\Delta v_y}{\Delta y_0} \frac{\Delta v_z}{\Delta z_0} + \Delta t \frac{\Delta v_x}{\Delta x_0} \frac{\Delta v_y}{\Delta y_0} \frac{\Delta v_z}{\Delta z_0} \right) \quad (2.10)$$

$$K_2 = \left(1 + \Delta t \frac{\Delta v_x}{\Delta x_0} \right) \left(1 + \Delta t \frac{\Delta v_y}{\Delta y_0} \right) \left(1 + \Delta t \frac{\Delta v_z}{\Delta z_0} \right) \quad (2.11)$$

where K_1 and K_2 are coefficients which respectively tend to zero and unity when Δt tends to zero. Eq (2.9) can be rewrite to:

$$\frac{D\rho}{Dt} + \rho \frac{\partial v_x}{\partial x} + \rho \frac{\partial v_y}{\partial y} + \rho \frac{\partial v_z}{\partial z} = 0 \quad (2.12)$$

or

$$\frac{D\rho}{Dt} + \rho \text{div}(\vec{v}) = 0 \quad (2.13)$$

While in geodynamics modelling, the density variations are small enough to be ignored, which is the result of Boussinesq approximation. The Boussinesq approximation assume that the density is linear proportional to the temperature and the small density variation is then neglected, except the gravity term.

$$\rho(T) = \rho_0 [1 - \alpha(T - T_0)] \quad (2.14)$$

where ρ_0 is the reference density at temperature T_0 and α is the volumetric thermal expansion coefficient. The boussinesq approximation also represent the incompressible condition, which mean the density of material points does no change with time. The incompressible continuity equation is broadly used in numerical geodynamic modelling, although on

many cases it is rather big simplification.

$$\nabla \cdot (\vec{v}) = 0 \quad (2.15)$$



Eq. (2.15) is the conservation of mass in our numerical modelling approach.

2.1.2 Motion—Conservation of momentum

In geodynamics, the time-dependent phenomena involve deformation of continuous media, which is the effect of the balance of internal and external forces that act in these media. So as to relate forces and deformation, an equation of motion may be used –The momentum equation. The momentum equation is a differential equivalent of Newton’ s second law to a continuous medium.

$$f = ma \quad (2.16)$$

f is the net force acting on the object and m is the mass of material. The momentum equation for a continuous medium in the gravity field: Eulerian Form:

$$\frac{\partial \sigma_{ij}}{\partial x_j} + \rho g_i = \rho \left(\frac{\partial v_i}{\partial t} + v_j \frac{\partial v_i}{\partial x_j} \right) \quad (2.17)$$

Lagrangian Form:

$$\frac{\partial \sigma_{ij}}{\partial x_j} + \rho g_i = \rho \frac{\partial D_{vi}}{\partial t} \quad (2.18)$$

While considering a small Lagrangian volume, the net force acting on the object

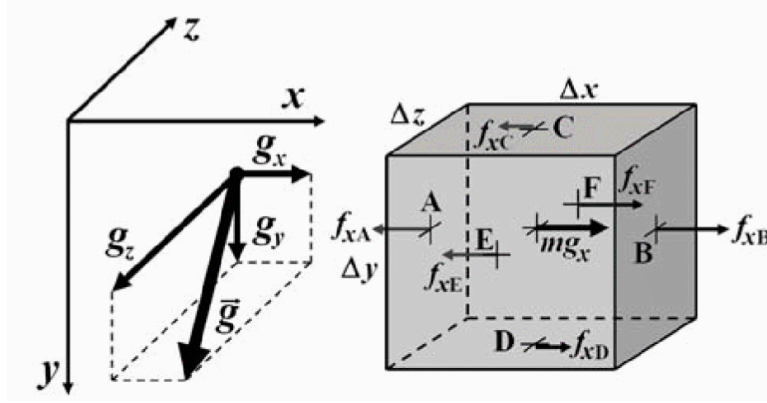


Figure 2.2: Lagrangian elementary Volume considered for the derivation of the respective form of x-momentum equation.

which can be computed locally. We will proof the momentum equation of Lagrangian Form below:

For x-component

$$f_x = f_{xA} + f_{xB} + f_{xC} + f_{xD} + f_{xE} + f_{xF} + mg_x \quad (2.19)$$

$f_{xA} - f_{xF}$ are stress-related forces, from the outside of the volume on the respective boundaries A-F. $f_g = m_g x$ is the gravity force.

$$f_{xA} = -\sigma_{xxA}\Delta y\Delta z \quad (2.20)$$

$$f_{xB} = +\sigma_{xxB}\Delta y\Delta z \quad (2.21)$$

$$f_{xC} = -\sigma_{xyC}\Delta x\Delta z \quad (2.22)$$

$$f_{xD} = +\sigma_{xyD}\Delta x\Delta z \quad (2.23)$$

$$f_{xE} = -\sigma_{xzE}\Delta x\Delta y \quad (2.24)$$

$$f_{xF} = +\sigma_{xzF}\Delta x\Delta y \quad (2.25)$$

We replace the force Eq(2.20-2.25) to Eq (2.19):

$$(\sigma_{xxB} - \sigma_{xxA})\Delta y\Delta z + (\sigma_{xyD} - \sigma_{xyC})\Delta x\Delta z + (\sigma_{xzF} - \sigma_{xzE})\Delta x\Delta y + mg_x = ma_x \quad (2.26)$$

Normalising both sides by considered Lagrangian volume

$$V = \Delta x\Delta y\Delta z \quad (2.27)$$

we obtain

$$\frac{(\sigma_{xxB} - \sigma_{xxA})\Delta y\Delta z}{V} + \frac{(\sigma_{xyD} - \sigma_{xyC})\Delta x\Delta z}{V} + \frac{(\sigma_{xzF} - \sigma_{xzE})\Delta x\Delta y}{V} + \frac{m}{V}g_x = \frac{m}{V}a_x \quad (2.28)$$

or

$$\frac{\Delta\sigma_{xx}}{\Delta x} + \frac{\Delta\sigma_{xy}}{\Delta y} + \frac{\Delta\sigma_{xz}}{\Delta z} + \rho g_x = \rho a_x \quad (2.29)$$

While the differences of the respective stresses components all tend to zero, we obtain:

$$\frac{\partial\sigma_{xx}}{\partial x} + \frac{\partial\sigma_{xy}}{\partial y} + \frac{\partial\sigma_{xz}}{\partial z} + \rho g_x = \rho a_x \quad (2.30)$$

or

$$\partial_j\sigma_{ij} + \rho g_i = \rho\ddot{u} \quad (2.31)$$

where u is the displacement.

2.1.3 Heat equation — Conservation of energy



To describe the balance of energy in a continuum material, heat equation is apply to measure the temperature change. The heat equation sloved the heat transport and porvided the temperature field. Below is the heat equation in Lagrangian form :

$$\rho C_p \frac{DT}{Dt} = -\frac{\partial q_x}{\partial x} - \frac{\partial q_y}{\partial y} - \frac{\partial q_z}{\partial z} + H_s + H_L \quad (2.32)$$

where ρ is the density, C_p is the heat capacity at constant pressure (isobaric heat capacity), H_s is shear heating and H_L is the latent heat production.

The proof of heat equation is show below:

Base on the Boussinesq approximation, the incompressible Lagrangian form governing equations are:

$$\nabla \cdot (\vec{v}) = 0 \frac{\partial \sigma_{ij}}{\partial x_j} + \rho g_i = \rho \frac{\partial D_{vi}}{\partial t} \rho C_p \frac{DT}{Dt} = -\frac{\partial q_x}{\partial x} - \frac{\partial q_y}{\partial y} - \frac{\partial q_z}{\partial z} + H_s + H_L \quad (2.33)$$

Describe conservation of mass, conservation of momentum and conservation of energy, respectively.

2.2 Finite elements method

finite elements method

2.3 Rheological behavior

****What is viscous and the viscous rheology of rock****

In the near-surface region, rocks undergo relatively low temperature and, therefore, the Earth's lithosphere easily result in brittle (at low pressure) and plastic (at high pressure) deformation. While in the deep earth, temperature increasing with depth, rocks behave viscous with irreversible deformation. Therefore, if a geodynamics model need to account for a wide range of rocks properties, it should consider the elasto-visco-plastic rheology of rocks.

Elastic rheology assume that the relationship between applied stress and strain is proportionality.

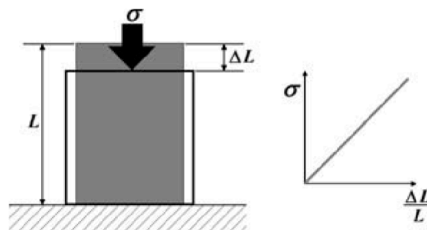


Figure 2.3: Elastic deformation

While plastic.....

Viscous rheology define....

2.4 Phase change

In this study, we use markers to trace the rocks phases, pressure and temperature. At the time the pressure and temperature satisfy the phase transformation condition, the marker will turns to new rock phase. A basalt element represent an element with more than 30 presents of the basalt phase markers. In this case, the element behave the deformation

as same as the basalt rheology.

2.4.1 Peridotite — Serpentine

Once the subducting plate sink into mantle, sediment on oceanic plate undergo higher pressure and temperature that release a large amount of fluids. On the other hand, the oceanic plate itself also carries seawater into the mantle. Fluids in subduction zone mostly concentrated in the mantle wedge. The dry mantle wedge undergo hydration process, lead to the transformation of peridotite to serpentine. The serpentine depth and thickness in subduction zone is not well understand since the seismic study constrain still contain high uncertainly, we model the phase transformation process of serpentine in parameter way.

Serpentine are stable in the colder mantle wedge relative to deeper mantle, and therefore once the serpentine under unstable field, we assume that serpentine rocks release fluid and transfer to peridotite. The following equations are the conditional expressions of serpentine—peridotite transformation. Figure is the phase diagram of mantle phases.

2.4.2 Basalt — Eclogite

As the oceanic crust sink into deeper mantle, the mafic rocks enters the eclogite stability field in the condition of high pressure. Therefore, basalt phases transform to eclogite. In this model, oceanic crust are tracked and compared with the eclogite stability filed, the following equations are the conditional expressions of mafic rocks transformation. Figure below is the mafic rocks phase diagram.



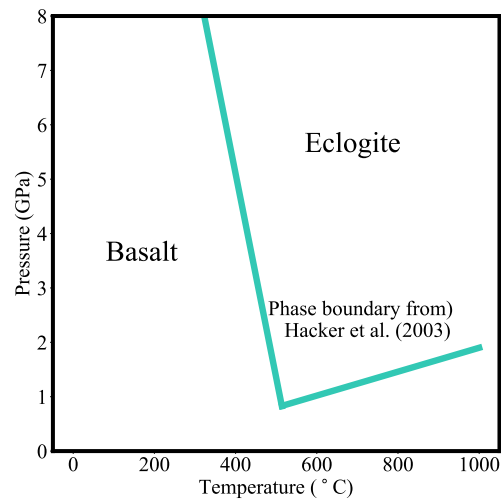


Figure 2.4: Phase diagram showing the stability field for mafic rocks (Hacker et al., 2003).

2.4.3 Sediment — Schist

Once sediment undergo higher pressure, the compression process and mataphase(變質作用)process occur. In this model, the following equations are the conditional expressions of transformation process of sediment to schist.

$$T > 650^{\circ}C$$

$$depth > 20km$$

The subducted sediments will turn into schist when temperature is greater than $650^{\circ}C$ and pressure is greater than (a number)

2.4.4 Hydrated olivine — Peridotite

We considering a hydrated peridotite under the oceanic crust in our model. The magma will only generated above the hydrated subducting oceanic lithosphere. Once the tempertaure is too high to make the rock contain water, the hydrated olivine transform to normal peridotite. The following equation is the conditional expression of this

transformation.

$$T > 800 - 35 \times 10^{-9} \times (\text{depth} - 62)^{2^{\circ}C}$$



2.5 Boundary condition

2.5.1 Kinematic boundary condition

2.5.2 Thermal boundary condition

For oceanic lithosphere, we used half space cooling model in our model to defined the thermal condition. The plate depth is proportional to the square root of oceanic lithosphere age, and therefore, the half space cooling model can predict well for the temperature of the oceanic plate. Follow by David and Lister, 1974(mention in Stein, 1995):

$$T = T_m \cdot \text{erf}\left(\frac{z}{2\sqrt{\kappa t}}\right)$$

T is the temperature, T_m is the mantle temperature, in this model the temperature is 1330 K, z is the depth from surface in kilometer and κ is the thermal diffusivity coefficient, that is, 10^{-6} in this study. t is the lithosphere age in Myr.

For continental lithosphere, the thermal condition is defined in linearly.

2.6 FLAC

We used the Fast Lagrangian Analysis of Continua (FLAC) technique. FLAC is a two-dimensional, explicit finite element with Lagrangian grid of numerical program.

What is explicit?

An explicit form is any solution that is given in the form $y = y(t)$. That is, y only

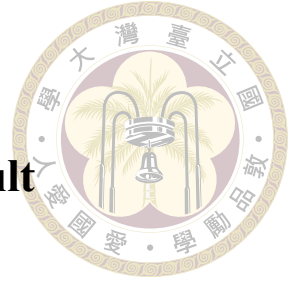
shows up once on the left hand side and is only in first power. On the other hand, implicit form is any solution that is not in explicit form. In finite element method, explicit solution solve the acceleration. In most cases, only the diagonal elements in matrix are not equal to zero, in other words, it is simple to solve an inversion solution form inverse matrix.

Gird?

2.7 Initial Model

initial model





Chapter 3 Numerical model result

3.1 Reference model

3.2 Flat subduction definition

3.3 Oceanic lithosphere

3.3.1 Oceanic plateau

3.3.2 Basalt transformation

3.4 Continental lithosphere

3.4.1 Thickness

3.4.2 Thermal state

3.4.3 lithosphere strength

3.5 Sublithosphere mantle

3.5.1 Viscosity

3.5.2 Serpentinization

3.5.3 410 discontinuity





Chapter 4 Discussion

4.1 Type of flat subduction

4.2 Magma sources of flat subduction

4.3 Serpentinization and observation

4.4 Flat subduction in Mexico

4.5 Flat subduction in Chile

4.6 Shallow angle subduction

This is just to test [?] the cite function.





Appendix A — Introduction

A.1 Introduction

A.2 Further Introduction

Appendix B — Introduction

B.1 Introduction

B.2 Further Introduction